Published version available at: https://doi.org/10.1016/j.proci.2022.07.065

Superadiabatic small-scale combustors: asymptotic analysis of a two-step chain-branching combustion model

Javier Bosch, Daniel Fernández-Galisteo, Carmen Jiménez, Vadim N. Kurdyumov

Department of Energy, CIEMAT, Avda. Complutense 40, 28040 Madrid, Spain

Abstract

An asymptotic study for a counterflow burner consisting of thin channels with heat exchange is proposed. The focus is made on the cases of ultra lean burning using a model of a two-step chain-branching chemistry. The ratio of the channel length to the thermal flame thickness is used as a natural large parameter. Then, the solution is constructed by the method of asymptotic expansions using this parameter. Finally, the obtained asymptotic for the flame position is satisfactorily compared with the exact solution of the problem. These explicit results have a clear advantage in that they facilitate considerably the parametric analysis. It is demonstrated that combustion of mixtures below the flammability limit can be carried out in the considered systems.

Keywords: Micro combustion; Narrow-channel approximation; Two-step kinetic model; Superadiabatic flames (8/10)

1. Introduction

The study of superadiabatic combustion devices has received noticeable attention recently, although the idea of carrying out combustion in these systems emerged a long time ago [1–3]. This attention is due to their ability to obtain a stable combustion process for mixtures with a low heat content allowing to burn fuel/air mixtures under the flammability limit or low grade fuels. Their defining property is the useful utilization of heat from combustion for preheating the cold initial mixture. Reviews of these devices can be found at [4–6].

The study of the flame structure and stability in superadiabatic burners has been mainly carried out within the framework of the one-step chemical Arrhenius model [7–13]. Despite an excellent qualitative and quantitative description of the combustion process, this model does not contain the essential ingredient needed to describe the combustion of lean mixtures. In the one-step Arrhenius model, there is no flammability limit for the mixture, namely, there is not a flame temperature below which combustion is impossible.

The simplest combustion kinetics containing a flammability limit includes the two-step chain-branching mechanism. This model was proposed in [14–16] and later developed in [17–21]. Subsequently, this mechanism was widely used to study various flame properties [22–28].

An analysis of a simplified counterflow microburner configuration using this chain-branching mechanism was recently presented in [29]. In that study the combustion process occurred only in one channel while the adjacent channel contained a neutral gas serving as a heat carrier. In the present paper, we propose an analysis of a more complex configuration, where the combustion process is considered in two counterflowing channels. Emphasis is made on studying the asymptotic cases corresponding to a long device, when its length is much greater than the thermal width of the flame. This technique allows to obtain explicit analytical expressions for the flame position and the conditions for its existence.

2. Mathematical formulation

A sketch of the microburner configuration investigated in the present study is shown in Fig. 1. The mixture of fuel and oxidizer flows in adjacent channels in the opposite directions. The initial temperature of both channels is equal to T_0 and the initial mass fraction of the combustible substance is F_0. The mixture is assumed to be deficient in fuel while the mass fraction of the oxidizer, which is in abundance, remains nearly constant. According to the diffusive-thermal model applied in the present study, the density of the mixture ρ, the heat capacity c_p, the thermal conductivity, λ, and the molecular diffusivities of the fuel and radical species in the mixture, $\mathcal{D}_F$, $\mathcal{D}_Z$, are all constant. $\mathcal{D}_T = \lambda/\rho c_p$ stands for the thermal diffusivity,

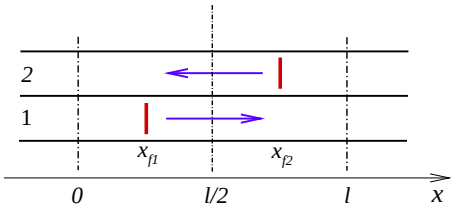

Fig. 1: Sketch of the microburner configuration. Heat exchange between the channels takes place within the segment $0 < x < \ell$. Arrows indicate gas flow directions and the vertical bold lines indicate flames located at x_{f_1} and x_{f_2}.

and is also constant within this model.

The channel system is assumed to be laterally periodic so that only two adjacent channels need to be considered in order to describe the steady-state solutions. The channels are also assumed to be thin enough to allow a one-dimensional model to be applied to describe the process [13]. Thermal exchange between the channels occurs within a segment of length L. As demonstrated in [29], for a sufficiently large length L, the model used to described the thermal conditions at $x < 0$ and $x > L$ becomes insignificant. In this study, we assume that heat transfer with the external environment outside the heat exchange segment is so fast that the temperature of the gas entering this segment is equal to the temperature of the external environment, which is equal to T_0.

The two-step chain-branching kinetic mechanism used in the present study is identical to that developed in [19–21]. This chemistry includes the autocatalytic reaction, $F + Z \to 2Z$, and the recombination reaction, $Z + M \to P + M + Q$, with reaction rates given by

$$\begin{aligned} \Omega_B &= A_B(\rho F/W_F)\cdot(\rho Z/W_Z)\, e^{-E/R_g T}, \\ \Omega_C &= A_C(\rho Z/W_Z)\cdot(\rho/W), \end{aligned} \qquad (1)$$

where Ω_B is the chain-branching reaction rate, assumed to be thermally sensitive with activation energy E, and Ω_C is the completion reaction rate with zero activation energy. As usual, all the heat, Q, is released in the completion step. In Eq. (1) A_B and A_C represent the reaction rate constants, ρ is the density, T is the temperature, F and Z are the mass fractions of fuel and radicals, R_g is the universal gas constant, and W_F, W_Z and W are the fuel, radical and mean molecular weights, respectively.

The main feature of this combustion model is the presence of a chain-branching crossover temperature, T_c, below which the rate of removal of the radical is larger than the rate of chain-branching. The crossover temperature T_c is determined by the relation $\Omega_B = \beta^2\Omega_C$ evaluated at the initial fuel mass fraction F_0, where $\beta = E(T_c - T_0)/R_g T_c^2$ is the Zel'dovich number based on T_c. It is important to see that the radical mass fractions Z in Ω_B and Ω_C are canceled out and, finally, T_c is defined by the equa-

tion

$$\frac{A_B}{A_C}\frac{W}{W_F}F_0 = \left\{\frac{E}{R_g}\cdot\frac{T_c-T_0}{T_c^2}\right\}^2 e^{E/R_gT_c}. \quad (2)$$

The characteristic time and length used to define the dimensionless variables, $x = \tilde{x}/L_c$ and $t = \tilde{t}/t_c$, are chosen from the following relations

$$t_c\,\mathcal{D}_T/L_c^2 = 1, \quad t_c\rho A_C/W = 1. \quad (3)$$

Using F_0 and $Z_0 = (W_Z/W_F)F_0$ to normalize the mass fractions of fuel and radicals, respectively, and the dimensionless temperature $\theta = (T-T_0)/(T_c - T_0)$, the steady-state dimensionless governing equations take the form

$$\pm m\,F_i^I = Le_F^{-1}\,F_i^{II} - \omega_i\,, \quad (4)$$

$$\pm m\,Z_i^I = Le_Z^{-1}\,Z_i^{II} + \omega_i\, - Z_i, \quad (5)$$

$$\pm m\,\theta_i^I = \theta_i^{II} + qZ_i \pm b\,(\theta_2-\theta_1)\,, \quad (6)$$

where the subscripts $i = 1$ and 2, together with the upper and lower signs in the equations, refer to the first and second channel, respectively, while f^I denotes the derivative of f with respect to x. The dimensionless reaction rate takes the form

$$\omega_i = \beta^2\,F_i\,Z_i\,\exp\left\{\frac{\beta(\theta_i-1)}{1+\gamma(\theta_i-1)}\right\}. \quad (7)$$

In Eqs. (4)-(6) b is the effective dimensionless coefficient of heat exchange between channels defined below, $\ell = L/L_c$ is the dimensionless length of the heat exchange segment, $m = U/U_c$ is the dimensionless flow velocity, $q = QF_0/c_p(T_c - T_0)W_F$ is the dimensionless heat of reaction, $\gamma = (T_c - T_0)/T_c$ is the heat release parameter and $Le_F = \mathcal{D}_T/\mathcal{D}_F$ and $Le_Z = \mathcal{D}_T/\mathcal{D}_Z$ are the Lewis numbers of the fuel and radicals. The critical value for the flammability limit within the model used, q_c, depends on β. In the limit $\beta \gg 1$, we have $q_c = 1$, see [29].

A linear model is used to simulate the process of heat exchange between channels, as in [13]. For thin channels, the final expression for b takes the form.

$$b = \alpha\frac{\lambda_w}{\lambda}\frac{L_c^2}{HH_w}\,, \quad (8)$$

where H and H_w are the channel and wall widths, respectively, and λ_w is the wall thermal conductivity. The value of the coefficient α depends on the configuration of the burner: if a periodic array of channels is considered, as is done in [13], then $\alpha = 2$. If we consider only two channels with thermally isolated lateral adiabatic walls, $\alpha = 1$.

According to the burner configuration under investigation, Eqs. (4) and (5) are considered for $-\infty < x < \infty$, while Eqs. (6) need to be solved only within $0 < x < \ell$. The following boundary conditions are applied for the mass fractions of fuel and radicals and for the temperature

$$\begin{array}{l} x\to-\infty:\ F_1 - 1 = F_2^I = Z_1 = Z_2 = 0\,, \\ x\to\infty:\ F_1^I = F_2 - 1 = Z_1 = Z_2 = 0\,, \end{array} \quad (9)$$

$$x = 0,\,\ell: \quad \theta_1 = \theta_2 = 0\,. \quad (10)$$

The flame positions, x_{f1} and x_{f2}, are defined below as the points where the temperature is equal to the branching temperature, $\theta_1(x_{f1}) = 1$ and $\theta_2(x_{f2}) = 1$. For finite values of β, these points are close to those where the corresponding radical mass fractions $Z_{1,2}$ reach their maximum values. In the high activation energy asymptotic limit (HAEA) considered below, these points coincide.

In what follows, we consider only the solutions that are symmetric with respect to the point $x = \ell/2$,

$$\begin{array}{c} \theta_2(x) = \theta_1(\ell - x)\,, F_2(x) = F_1(\ell - x)\,, \\ Z_2(x) = Z_1(\ell - x)\,. \end{array} \quad (11)$$

Thus, the flame positions in the first and second channels are also located symmetrically with respect to $x = \ell/2$, i.e. $x_{f2} = \ell - x_{f1}$. For this reason, in order to characterize the state of the system, it is sufficient to describe the flame position and the distributions of variables in the first channel. The corresponding index will be omitted for brevity. Thus, x_f will be used below instead of x_{f1} when it does not cause confusion.

When looking for symmetric distributions, two flame configurations should be considered. In the first case, the flame in the first channel is located at $0 < x_{f1} < \ell/2$, and, respectively, $\ell/2 < x_{f2} < \ell$. In the second case, $\ell/2 < x_{f1} < \ell$ and $0 < x_{f2} < \ell/2$ are assumed. In both cases, it is sufficient to consider only half of the channel using the symmetry conditions derived from Eq. (11)

$$x = \ell/2: \quad f_1 = f_2, \quad f_1^I = -f_2^I\,, \quad (12)$$

where f stands for θ, F or Z.

3. Asymptotic analysis

3.1. High activation energy limit $\beta \gg 1$

Within the HAEA limit, the radical production term is reduced for $\beta \gg 1$ to the Dirac δ-function, namely $\omega \sim \delta(x - x_f)$, with x_f located at the point where the temperature is equal to the dimensionless branching temperature, see [19–21]. The standard jump conditions for variables across the flame sheet take the form

$$\left[Z_1\right] = \left[F_1\right] = Le_F^{-1}\left[F_1^I\right] + Le_Z^{-1}\left[Z_1^I\right] = 0, \quad (13)$$

$$\theta_1|_{x_f\pm0} = 1,\ \left[\theta_2\right] = \left[\theta_1^I\right] = \left[\theta_2^I\right] = 0\,, \quad (14)$$

where $[f] = f(x_f + 0) - f(x_f - 0)$. These jump conditions are obtained by combining Eqs. (4)-(5) and integrating over the flame sheet.

Assuming that at $x = x_f$ the fuel is consumed completely, the solution of Eqs. (4)-(5) takes the form

$$F_1 = \begin{cases} 1 - \exp\left[Le_F\, m(x - x_f)\right], & x < x_f, \\ 0, & x > x_f, \end{cases} \tag{15}$$

$$Z_1 = \begin{cases} Z_f \exp[a_m(x - x_f)], & x < x_f, \\ Z_f \exp[a_p(x - x_f)], & x > x_f, \end{cases} \tag{16}$$

where

$$\begin{aligned} a_m &= (Le_Z\, m + \sqrt{Le_Z^2 m^2 + 4Le_Z})/2\,, \\ a_p &= (Le_Z\, m - \sqrt{Le_Z^2 m^2 + 4Le_Z})/2\,, \end{aligned} \tag{17}$$

and

$$Z_f = \frac{mLe_Z}{(Le_Z^2 m^2 + 4Le_Z)^{1/2}} \tag{18}$$

is obtained from the derivatives jump conditions given by Eq. (13). It can be checked from Eq. (16) that the mass fraction of radicals satisfies $\int\limits_{-\infty}^{\infty} Z_1\, dx = m$.

Finally, the problem of determining the steady-state temperature distributions and the flame positions is reduced to solving

$$\begin{cases} m\theta_1^I = \theta_1^{II} + qZ_1 - b\,(\theta_1 - \theta_2)\,, \\ -m\theta_2^I = \theta_2^{II} + qZ_2 + b\,(\theta_1 - \theta_2)\,, \end{cases} \tag{19}$$

with the boundary conditions given by Eq. (10), where Z_1 is determined by Eq. (16) and $Z_2(x) = Z_1(\ell - x)$.

In what follows, we first consider the cases with $\ell \gg 1$. Analysis shows that the cases with $m = \mathcal{O}(1)$ and $m \ll 1$ should be considered separately.

3.2. Results for $\ell \gg 1$ and $m = \mathcal{O}(1)$

Consider the limit of a long heat-exchange segment, $\ell \gg 1$. Estimates of the heat exchange parameter between the channels, b, suggest that it is small compared with unity. To carry out the asymptotic analysis, it is convenient to assume (formally) that $b = \tilde{b}/\ell$, where $\tilde{b} = \mathcal{O}(1)$.

To solve Eqs. (19) for $\ell \gg 1$ and $m = \mathcal{O}(1)$, the well known method of matched asymptotic expansions is applied. The procedure for finding a solution presented below is similar to that described in [29]. As usual, the inner and outer variables are introduced as follows: $\eta = x - x_f$ for the inner variable and $\xi = (x - x_f)/\ell$ for the outer variable. The flame position in the first channel, written in terms of an external variable, becomes $\xi_f = x_f/\ell$. The internal and external temperatures in two channels are denoted as $\theta_i^{in}(\eta)$ and $\theta_i^{out}(\xi)$, respectively, where $i = 1, 2$.

We have $|\eta| = \mathcal{O}(1)$ in the inner region. Taking into account that $b = \tilde{b}/\ell$, the heat-exchange term is small here, to the leading order. Thus, the solution of Eqs. (19) for $\theta_1^{in}(\eta)$ is given by

$$\theta_1^{in} = \begin{cases} c_1 + c_2 e^{m\eta} + \dfrac{qZ_f}{ma_m - a_m^2} e^{a_m \eta}, & \eta < 0\,, \\ c_3 + c_4 e^{m\eta} + \dfrac{qZ_f}{ma_p - a_p^2}\, e^{a_p \eta}, & \eta > 0\,, \end{cases} \tag{20}$$

where a_p, a_m and Z_f are determined by Eqs. (17)-(18).

Rewriting this inner solution in terms of the outer variable $\xi = \mathcal{O}(1)$ indicates that $c_4 = 0$ in order to eliminate the corresponding exponentially large term, $\sim c_4 e^{\ell\, m\, \xi}$ growing exponentially for positive $\xi = \mathcal{O}(1)$ and $\ell \gg 1$. Applying conditions (14) written at $\eta = 0$,

$$\theta_1^{in}(0+) = \theta_1^{in}(0-) = 1, \quad [d\theta_1^{in}/d\eta] = 0\,,$$

gives

$$\begin{aligned} c_1 &= 1 - \frac{qZ_f}{m}\left\{\frac{m - a_m}{ma_m - a_m^2} + \frac{a_p}{ma_p - a_p^2}\right\} \\ c_2 &= \frac{qZ_f}{m}\left\{\frac{a_p}{ma_p - a_p^2} - \frac{a_m}{ma_m - a_m^2}\right\} \\ c_3 &= 1 - \frac{qZ_f}{ma_p - a_p^2} \end{aligned} \tag{21}$$

Thus, from Eq. (20) it follows that

$$\lim_{\eta \to -\infty} \theta_1^{in}(\eta) = \theta_1^{(-)}, \quad \lim_{\eta \to +\infty} \theta_1^{in}(\eta) = \theta_1^{(+)}\,, \tag{22}$$

where $\theta_1^{(-)} = c_1$ and $\theta_1^{(+)} = c_3$. We have also that $\theta_1^{(+)} - \theta_1^{(-)} = q$, as it should be, and $\theta_1^{(-)} < 1$ and $\theta_1^{(+)} > 1$. These values are used for the matching procedure between the inner and outer solutions. In particular,

$$\theta_1^{(-)} = 1 - D \cdot q\,, \tag{23}$$

where

$$D = \frac{4Le_Z(m + s)}{s(Le_Z\, m + s)(2m - Le_Z\, m + s)} \tag{24}$$

with $s = \sqrt{Le_Z(Le_Z m^2 + 4)}$.

The leading order of Eqs. (19) written in terms of the outer variable takes the form

$$\begin{aligned} m\, d\theta_1^{out}/d\xi &= -\tilde{b}(\theta_1^{out} - \theta_2^{out})\,, \\ -m\, d\theta_2^{out}/d\xi &= \tilde{b}(\theta_1^{out} - \theta_2^{out})\,, \end{aligned} \tag{25}$$

because the radicals mass fraction given by Eq. (16) is exponentially small in the outer region $\xi = \mathcal{O}(1)$. For the matching of internal and external expansions, it is necessary to impose

$$\begin{aligned} \lim_{\xi \to 0-} \theta_1^{out}(\xi) &= \lim_{\eta \to -\infty} \theta_1^{in}(\eta)\,, \\ \lim_{\xi \to 0+} \theta_1^{out}(\xi) &= \lim_{\eta \to \infty} \theta_1^{in}(\eta)\,. \end{aligned} \tag{26}$$

The temperature in the adjacent channel is continuous at the point $\xi = 0$.

The general solution of Eqs. (25) has the form

$$\theta_1^{out}(\xi) = \frac{C_1 + C_2}{2} - \frac{\tilde{b}}{m}\, C_1 \xi, \qquad \theta_2^{out}(\xi) = \frac{C_2 - C_1}{2} - \frac{\tilde{b}}{m}\, C_1 \xi\,, \tag{27}$$

where C_1 and C_2 are arbitrary constants. As stated above, there are two cases to be considered.

Consider the case with $0 < \xi_f < 1/2$. The corresponding boundary and matching conditions are

$$\theta_1^{out}(-\xi_f) = 0, \quad \theta_2^{out}(0+) = \theta_2^{out}(0-)\,, \quad \lim_{\xi\to 0-} \theta_1^{out}(\xi) = \theta_1^{(-)}, \lim_{\xi\to 0+} \theta_1^{out}(\xi) = \theta_1^{(+)}, \quad \theta_1^{out}(1/2 - \xi_f) = \theta_2^{out}(1/2 - \xi_f). \tag{28}$$

Thus, there are four arbitrary constants (two on each side of the flame) appearing in Eq. (27) which are found by means of any four conditions from (28). The last fifth condition is used to determine the flame position ξ_f. A similar procedure for finding a solution is applied for the case where $1/2 < \xi_f < 1$.

After completing these algebraic steps, the solution for the flame position (in the first channel), written in terms of $x_f = \ell\xi_f$, takes the form

$$x_f = \begin{cases} m\theta^{(-)}/bq & \text{for} \quad 0 < x_f < \ell/2\,, \\ \ell - m\theta^{(-)}/bq & \text{for} \quad \ell/2 < x_f < \ell\,, \end{cases} \tag{29}$$

where $\theta_1^{(-)}$ is given by Eq. (23).

We note parenthetically that the external solution given by Eq. (27) for θ_2 does not satisfy the zero condition at $x = 0$, as required by Eq. (10). A similar situation occurs for the temperature θ_1 at $x = \ell$. In fact, from the point of view of the external solution, two boundary layers must be introduced: the first adjacent to $\xi = 0$ for θ_2 and the second for θ_1 adjacent to $\xi = \ell$. Nevertheless, after analyzing Eq. (19) for $\ell \gg 1$, the solutions within these boundary layers are trivially written in terms of the variable x in the form

$$x = \mathcal{O}(1):\ \theta_2 = \theta_2^{out}|_{\xi=0} \cdot [1 - e^{-mx}]\,, \quad x - \ell = \mathcal{O}(1):\ \theta_1 = \theta_1^{out}|_{\xi=1} \cdot [1 - e^{m(x-\ell)}]\,, \tag{30}$$

because the heat exchange term, of order ℓ^{-1}, is negligible here. In any case, the presence of these boundary layers does not affect in any way the final result for x_f given by of Eq. (29).

One can see from Eq. (29) that $x_f \to 0$ at $m \to 0$, that is, the flame approaches the cold inlet at low flow rates, which contradicts the physics of the process. Thus, the case of small m should be considered separately.

3.3. Results for $\ell \gg 1$ and $m \ll 1$

When obtaining Eqs. (25) written in terms of the external variable ξ, it was assumed that for $\ell \gg 1$ the diffusion term in the temperature equation, of order $1/\ell^2$, becomes small in comparison with the convective term, of order m/ℓ. This allowed us to apply the method of matched asymptotic expansions. This is not the case when $m \ll 1$.

Let us assume that $m = \tilde{m}/\ell$, where $\tilde{m} = O(1)$. It turns out that for $\ell \gg 1$ the asymptotic solution can be obtained by means of the regular expansion method using ℓ^{-1} as a small parameter. It is convenient to use the variable $\xi = x/\ell$. When doing this, the mass fraction of radicals in Eq. (19) acts formally as a δ-function. Indeed, writing the expression given by Eq. (16) for $m = \tilde{m}/\ell \ll 1$ in terms of the external variable results in

$$Z_1 = \frac{\tilde{m}\, Le_Z^{1/2}}{2\ell} \begin{cases} \exp\{Le_Z^{1/2}(\xi - \xi_f)\ell\}\,, & \xi < \xi_f, \\ \exp\{-Le_Z^{1/2}(\xi - \xi_f)\ell\}\,, & \xi > \xi_f, \end{cases} \tag{31}$$

in the fist approximation. One can see that the nonzero values of Z_1 take place within a narrow interval of width ℓ^{-1} around ξ_f. On the other side $\int\limits_{-\infty}^{\infty} Z_1 d\xi = \tilde{m}/\ell^2$. Thus, we have that $Z_1 \to \tilde{m}\delta(\xi - \xi_f)/\ell^2$ as $\ell \to \infty$.

Consider the case with $0 < \xi_f < 1/2$ for which $Z_2 \equiv 0$ in the first half of the heat exchange segment. Eqs. (19) written in terms of the variable ξ become

$$\begin{cases} \dfrac{\tilde{m}}{\ell^2}\dfrac{d\theta_1}{d\xi} = \dfrac{1}{\ell^2}\dfrac{d^2\theta_1}{d\xi^2} + \dfrac{q\tilde{m}}{\ell^2}\,\delta(\xi - \xi_f) - \dfrac{\tilde{b}}{\ell}\,(\theta_1 - \theta_2), \\ -\dfrac{\tilde{m}}{\ell^2}\dfrac{d\theta_2}{d\xi} = \dfrac{1}{\ell^2}\dfrac{d^2\theta_2}{d\xi^2} + \dfrac{\tilde{b}}{\ell}\,(\theta_1 - \theta_2), \end{cases} \tag{32}$$

to be solved for $0 < \xi < 1/2$. We can search a solution using a regular asymptotic expansion in the form

$$\begin{cases} \theta_1 = \theta_1^{(0)} + \ell^{-1}\theta_1^{(1)} + \dots\,, \\ \theta_2 = \theta_2^{(0)} + \ell^{-1}\theta_2^{(1)} + \dots\,. \end{cases} \tag{33}$$

One can see that the leading heat exchange term in Eq. (32) is of order ℓ^{-1}. Thus, we have $\theta_1^{(0)} = \theta_2^{(0)} = \theta^{(0)}$ as $\ell \gg 1$ within the interval $0 < \xi < 1/2$, in the first approximation. Summation of Eqs. (32) yields

$$\frac{d^2\theta^{(0)}}{d\xi^2} + \frac{1}{2} q\tilde{m}\,\delta(\xi - \xi_f) = 0\,, \tag{34}$$

to be solved subject to

$$\theta^{(0)}|_{\xi=\xi_f} = 1,\ \theta^{(0)}|_{\xi=0} = 0,\ d\theta^{(0)}/d\xi|_{\xi=1/2} = 0\,. \tag{35}$$

It should be remembered that, by definition, at the flame point, ξ_f, the temperature is equal to unity.

The solution of Eqs. (34)-(35) becomes

$$\theta = \begin{cases} \xi/\xi_f, & \xi < \xi_f, \\ 1, & \xi_f < \xi < 1/2. \end{cases} \tag{36}$$

Substitution of this expression into the condition required by the δ-function in Eq. (34), namely

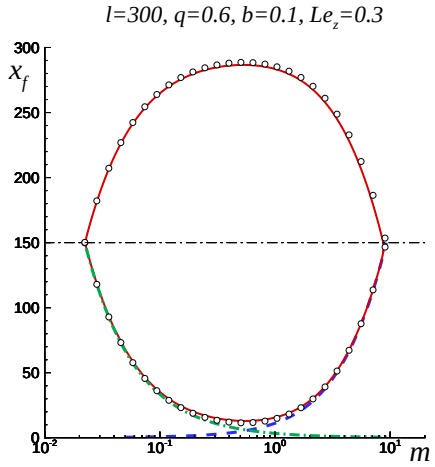

Fig. 2: Comparison of various asymptotic solutions for $\ell = 300$, $q = 0.6$, $b = 0.1$ and $Le_Z = 0.3$: dashed line - Eq. (29) for $m = \mathcal{O}(1)$, for $x_f < \ell/2$; dash-dotted line - Eq. (37) for $m \ll 1$, for $x_f < \ell/2$; open circles - composite solution given by Eq. (38); the solid curve shows the result of calculations at finite ℓ based on Eq. (39).

$[d\theta/d\xi] + q\tilde{m}/2 = 0$, provides an additional condition to determine ξ_f. The case with $1/2 < \xi_f < 1$ is considered similarly.

The final expression for the flame position for $m \ll 1$ written in terms of $x_f = \ell\xi_f$ takes the form

$$x_f = \begin{cases} 2/qm, & \text{for} \quad 0 < x_f < \ell/2, \\ \ell - 2/qm, & \text{for} \quad \ell/2 < x_f < \ell. \end{cases} \qquad (37)$$

It can be seen from Eq. (37) that as $m \to 0$ the flame position x_f moves away from the entrance to the heat exchange segment where the cold mixture enters, as it should be.

3.4. Composite solution for x_f

The solutions provided by Eq. (29) and Eq. (37) show that $x_f \to 0$ as $m \ll 1$ and that $x_f \to 0$ as $m \gg 1$, respectively. This allows to construct the first order composite expansion by combining Eq. (29) and Eq. (37) for x_f in the form

$$x_f = \begin{cases} \dfrac{m\theta_1^{(-)}}{b\,q} + \dfrac{2}{m\,q}, & 0 < x_f < \ell/2, \\ \ell - \left(\dfrac{m\theta_1^{(-)}}{b\,q} + \dfrac{2}{m\,q}\right), & \ell/2 < x_f < \ell, \end{cases} \qquad (38)$$

where $\theta_1^{(-)}$ is given by Eq. (23).

4. Comparison with finite-ℓ results

In order to validate the results presented above, Eqs. (19) were solved analytically for large but finite values of ℓ following the procedure presented in [29]. The symmetric solutions were sought separately for $0 < x_f < \ell/2$ and for $\ell/2 < x_f < \ell$.

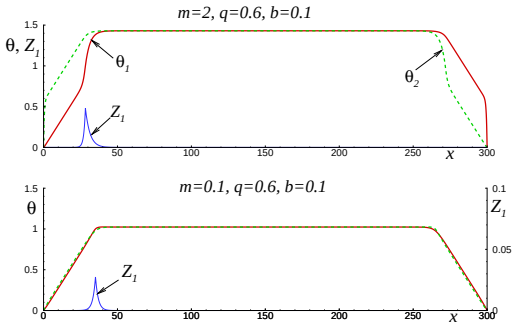

Fig. 3: Solutions obtained with finite ℓ; θ_1 - solid line, θ_2 - dashed line, Z_1 - thin solid line, all curves for $\ell = 300$, $q = 0.6$ and $b = 0.1$; upper plot for $m = 2$, lower plot for $m = 0.1$.

Equations (19) written on both sides of the flame sheet are linear and have an analytical solution containing eight constants, $\{C_i,\ i = 1, \ldots 8\}$, four on each side. These constants are determined from any eight conditions given by Eqs. (10) and (14), which requires solving a system of eight linear inhomogeneous equations. The remaining ninth condition providing a solvability condition of the form

$$\mathcal{F}(x_f; m, q, \ell, b, Le_Z) = 0 \qquad (39)$$

is applied to determine the flame position, x_f. All steps were carried out by means of MAPLE facilities. The resulting analytical expression for the function $\mathcal{F}$ is too long to be given here explicitly. After that, the roots of Eq. (39) were found numerically.

Figure 2 compares the asymptotic curves for $\ell \gg 1$ with analytical results obtained for finite ℓ, all curves for $\ell = 300$, $q = 0.6$, $b = 0.1$ and $Le_Z = 0.3$. The dashed and dash-dotted curves show Eq. (29) for $m = \mathcal{O}(1)$ and Eq. (37) for $m \ll 1$, respectively, both plotted for only for $x_f < \ell/2$. Open circles and a solid line represent the composite expansion given by Eq. (38) and the flame position calculated for finite ℓ using Eq. (39). Good agreement can be seen which confirms the possibility of using these asymptotic results for the analysis of a superadiabatic device.

Figure 3 compares the flame soltions with $m = 2$ (upper plot) and $m = 0.1$ (lower plot) showing the temperature distributions in both channels, θ_1 and θ_2, and the mass fraction of radicals Z_1 (only in the first channel) calculated for $\ell = 300$. The flame position was calculated from Eq. (39) for the case with $0 < x_f < \ell/2$. The temperature and mass fraction solutions computed using Eqs. (19) are plotted for $q = 0.6$, $b = 0.1$ and $Le_Z = 0.3$.

In the upper plot of Fig. 3, it can be seen that the temperature distributions are linear outside the region of nonzero Z_1, which corresponds to the external solution given by Eq. (27). The interval of x where Z_1

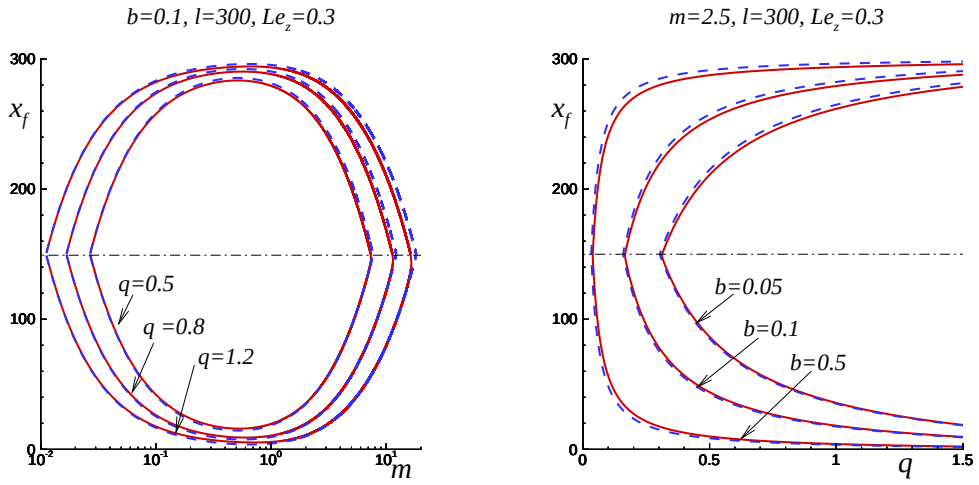

Fig. 4: Comparison of flame positions x_f as functions of the flow rate m (left plot) and the heat of reaction q (right plot) obtained from Eq. (39) for finite ℓ (solid lines) and the asymptotic composite solution given by Eq. (38) (dashed lines), for $\ell = 300$ and $Le_Z = 0.3$.

has nonzero values corresponds to the internal region described by Eq. (20). One can see also the boundary layers at $x = 0$ for θ_2 and at $x = \ell$ for θ_1, where the corresponding temperatures drop to zero, as indicated by the solution given by Eq. (30). The lower plot of Fig. 3 shows that for $m \ll 1$ the difference between θ_1 and θ_2 is small everywhere, as follows from Eq. (33) for large ℓ.

Figure 4 shows a comparison between the analytical solution for finite values of ℓ based on the numerical solution of Eq. (39) (solid curves) and the asymptotic composite solution given by Eq. (38) (dashed curves). The left figure shows the dependencies for x_f on m for several values of q, the right figure shows the dependence for x_f on q for $m = 2.5$ and several values of b. It can be seen that the asymptotic solution gives a good approximation for the flame position as well as for the critical values of the flow rate or the heat of reaction. The authors wish to emphasize that the mixtures with $q < 1$ are below the flammability limit. However, Fig. 4 shows that combustion is feasible for these mixtures in this type of devices.

The study of the stability of the found steady-state regimes is beyond the scope of the present work. However, previous studies based on various models for superadiabatic devices indicate that only the solutions corresponding to the lower branch of x_f are stable, see [8, 29].

It should also be noted that the right-hand side of Eq. (38) for x_f does not depend on ℓ. To determine the critical value of any parameter, such as, for example, the minimal reaction heat value, q_{min}, above which the flame exists, it is necessary to equate x_f to $\ell/2$ in Eq. (38) (given that this flame position corresponds to the critical point). In particular, we have

$$q_{min} = \left(\frac{m}{b} + \frac{2}{m}\right) \Big/ \left(\frac{m}{b} D + \frac{\ell}{2}\right), \qquad (40)$$

where D is given by Eq. (24).

5. Conclusions

Determining the rank of parameter values at which a given device has an operating mode is a key task in the design and utilization of a device. This can be done only on the basis of a mathematical model for the process, which usually contains a large number of parameters. These parameters describe the chemical kinetics of the process, the geometric device features, its thermo-physical properties, and so on. The mathematical model itself is usually built on the basis of differential equations describing conservation laws for the energy and mass of reacting substances. The parametric analysis of the resulting model often faces certain difficulties, such as the multiplicity of the solutions. In view of these circumstances, the asymptotic analysis is a convenient tool often even leading to explicit expressions thus facilitating the parametric study.

In this investigation, an asymptotic analysis is presented for a superadiabatic counterflow burner using a chain-branching combustion chemistry model. In the analysis, the channels where combustion takes place are assumed to be sufficiently thin, which allows a one-dimensional flow description. In the considered cases, the length of the channels is chosen significantly greater than the thermal flame thickness providing a large natural parameter of the problem.

When doing the asymptotic expansions of the differential equations using this parameter, the channel must be divided into two regions: the reaction zone and the convective zone. Explicit solutions are obtained in each zone and the matching of the corresponding solutions provides an explicit expression for determining the flame position. The resulting explicit asymptotic solution has been compared satisfactorily with the exact solution of the problem estimated at large but finite values of the expansion parameter. The latter reveals that the asymptotic method provides a good approximation for the solutions. The main result of this work is a demonstration of the possibility to ensure the combustion process for mixtures below the flammability limit in superadiabatic devices of the considered type.

Acknowledgments

This work was financed by project #PID2019-108592RB-C42 MCIN / AEI / 10.13039/ 501100011033.

References

[1] S.A. Lloyd, F.J. Weinberg, A burner for mixtures of very low heat content, *Nature* 251 (1974) 47-49.

[2] S.A. Lloyd, F.J. Weinberg, Limits to energy release and utilisation from chemical fuels, *Nature* 257 (1975) 367-370.

[3] A.R. Jones, S.A. Lloyd, F.J. Weinberg, Combustion in heat exchangers, *Proc. R. Soc. Lond. A.* 360 (1978) 97-115.

[4] A.C. Fernández-Pello, Micropower generation using combustion: issues and approaches, *Proc. Combust. Inst.* 29 (2002) 883-899.

[5] Y. Ju, K. Maruta, Microscale combustion: technology development and fundamental research, *Prog. Energy Combust. Sci.* 37 (2011) 669-715 .

[6] J.L. Ellzey, E.L. Belmont, C.H. Smith, Heat recirculating reactors: Fundamental research and applications, *Prog. Energy Combust. Sci.* 72 (2019) 32-58.

[7] Y. Ju, C.W. Choi, An analysis of sub-limit flame dynamics using opposite propagating flames in mesoscale channels, *Combust. Flame* 133 (2003) 483-493.

[8] R.V. Fursenko, S. S. Minaev, Flame stability in a system with counterflow heat exchange, *Combust. Explos. Shock Waves* 41(2) (2005) 133-139.

[9] I. Schoegl, J.L. Ellzey, Superadiabatic combustion in conducting tubes and heat exchangers of finite length, *Combust. Flame* 151 (2007) 142-159.

[10] V.N. Kurdyumov, M. Matalon, Analysis of an idealized heat-recirculating microcombustor, *Proc. Combust. Inst.*, 33(2) (2011) 3275-3284.

[11] M. Sánchez-Sanz, Premixed flame extinction in narrow channels with and without heat recirculation, *Combust. Flame* 159 (2012) 3158-3167.

[12] E. Fernández-Tarrazo, M. Sánchez-Sanz, R. Fursenko, S. Minaev, Multiple combustion regimes and performance of counter-flow microcombustor with power extraction, *Math. Modell. Nat. Phen.* 13 (2018) UNSP 52.

[13] V.N. Kurdyumov, D. Fernández-Galisteo, C. Jiménez, Superadiabatic small-scale combustor with counterflow heat exchange: Flame structure and limits to narrow-channel approximation, *Combust. Flame* 222 (2020) 233-241.

[14] Ya.B. Zeldovich, K teorii rasprostranenia plameni, *Zh. Fiz. Khim.* 22 (1948) 27-48; Theory of flame propagation, English translation: *Nat. Advis. Comm. Aeronaut.* Technical Memorandum No. 1282, 1951.

[15] Ya.B. Zeldovich, G.I. Barenblatt, Theory of Flame Propagation, *Combust. Flame* 3 (1959) 61-74.

[16] Ya.B. Zeldovich, Chain reactions in hot flames - an approximate theory for flame velocity, *Kinetika i kataliz* 2 (1961) 305-318; English translation: *Int. Chem. Eng.* 2 (1962) 227-235.

[17] A. Liñán, A theoretical analysis of premixed flame propagation with an isothermal chain-branching reaction, Insituto Nacional de Technica Aerospacial Esteban Terradas (Madrid), USAFORS Contract No. E00AR68-0031, Technical Report No. 1, 1971.

[18] G. Joulin, A. Liñán, G.S.S. Ludford, N. Peters, C. Schmidt-Laine, Flames with chain-branching/chain-breaking kinetics, *SIAM J. Appl. Math.* 45 (1985) 420-434.

[19] J.W. Dold, R.W. Thatcher, A. Omon-Arancibia, J. Redman, From one-step to chain-branching premixed flame asymptotics, *Proc. Combust. Inst.* 29 (2002) 1519-1526.

[20] J.W. Dold, R.O. Weber, R.W. Thatcher, A.A. Shah, Flame balls with thermally sensitive intermediate kinetics, *Combust. Theory Modell.* 7 (2003) 175-203.

[21] J.W. Dold, Premixed flames modelled with thermally sensitive intermediate branching kinetics, *Combust. Theory Modell.* 11 (2007) 909-948.

[22] V.V. Gubernov, H.S. Sidhu, G.N. Mercer, Combustion waves in a model with chain branching reaction and their stability, *Combust. Theory Modell.* 12 (2008) 407-431.

[23] V.V. Gubernov, H.S. Sidhu, G.N. Mercer, A.V. Kolobov, A.A. Polezhaev, The effect of Lewis number variation on combustion waves in a model with chain-branching reaction, *Math. Chem.* 44 (2008) 816-830.

[24] V.V. Gubernov, A.V. Kolobov, A.A. Polezhaev, H.S. Sidhu, G.N. Mercer, Pulsation instabilities of combustion waves in a chain-branching reaction model, *I. J. Bif. Chaos* 19 (2009) 873-887.

[25] G.J. Sharpe, Effect of thermal expansion on the linear stability of planar premixed flames for a simple chain-branching model: The high activation energy asymptotic limit, *Combust. Theory Modell.*, 12 (2008) 717-738.

[26] G.J. Sharpe, Thermal-diffusive instability of premixed flames for a simple chain-branching chemistry model with finite ectivation energy, *SIAM J. Appl. Math.* 70 (2009) 866-884.

[27] V.V. Gubernov, A.V. Kolobov, A.A. Polezhaev, H.S. Sidhu, Stability of combustion waves in the Zeldovich-Liñán model, *Combust. Flame* 159 (2012) 1185-1196.

[28] V.N. Kurdyumov, D. Fenández-Galisteo, Asymptotic structure of premixed flames for a simple chain-branching chemistry model with finite activation energy near the flammability limit, *Combust. Flame* 159 (2012) 3110-3118.

[29] J. Bosch, D. Fernández-Galisteo, C. Jiménez, V.N. Kurdyumov, Analytical study of superadiabatic small-scale combustors with a two-step chain-branching chemistry model: lean burning below the flammability limit, *Combust. Flame* 235, (2022) 11173.